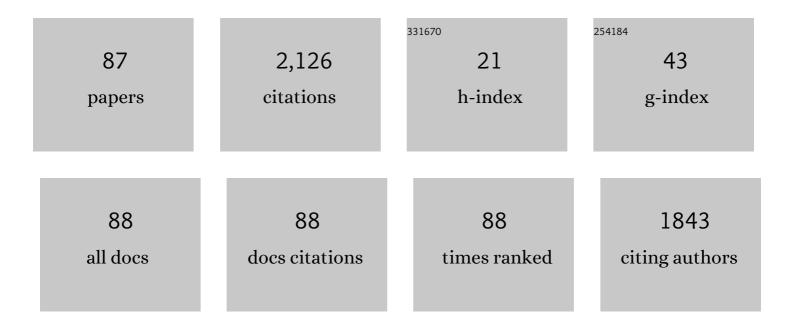
Hou-Bing Huang

List of Publications by Year in descending order

Source: https://exaly.com/author-pdf/6226792/publications.pdf Version: 2024-02-01



#	Article	IF	CITATIONS
1	Phase Diagram of Subâ€GHz Electricâ€Fieldâ€Induced Polarization Oscillation. Physica Status Solidi - Rapid Research Letters, 2022, 16, 2100416.	2.4	6
2	Phase-Field Simulation of Superconductor-Ferromagnet Bilayer-Based Cryogenic Strain Sensor. Journal of Superconductivity and Novel Magnetism, 2022, 35, 409-414.	1.8	2
3	Microscopic physical origin of polarization induced large tunneling electroresistance in tetragonal-phase BiFeO3. Acta Materialia, 2022, 225, 117564.	7.9	6
4	Selfâ€Assembled Epitaxial Ferroelectric Oxide Nanospring with Superâ€Scalability. Advanced Materials, 2022, 34, e2108419.	21.0	11
5	Understanding electrocaloric cooling of ferroelectrics guided by phaseâ€field modeling. Journal of the American Ceramic Society, 2022, 105, 3689-3714.	3.8	17
6	Tip-Induced In-Plane Ferroelectric Superstructure in Zigzag-Wrinkled BaTiO ₃ Thin Films. Nano Letters, 2022, 22, 2859-2866.	9.1	11
7	Phase-field simulations of vortex chirality manipulation in ferroelectric thin films. Npj Quantum Materials, 2022, 7, .	5.2	22
8	Strain Engineering of Energy Storage Performance in Relaxor Ferroelectric Thin Film Capacitors. Advanced Theory and Simulations, 2022, 5, .	2.8	13
9	Selfâ€Assembled Epitaxial Ferroelectric Oxide Nanospring with Super‣calability (Adv. Mater. 13/2022). Advanced Materials, 2022, 34, .	21.0	0
10	Pressure-induced room temperature electrocaloric effect in BiFeO3-PbTiO3 solid solution based on Landau-Devonshire theory. Materials Today Communications, 2022, 31, 103396.	1.9	2
11	Ultrafast Ferroelectric Domain Switching Induced by Nanoâ€Second Strainâ€Pulse. Advanced Theory and Simulations, 2022, 5, .	2.8	10
12	Photoenhanced Electroresistance at Dislocation-Mediated Phase Boundary. ACS Applied Materials & Interfaces, 2022, 14, 18662-18670.	8.0	3
13	Simultaneously achieving giant piezoelectricity and record coercive field enhancement in relaxor-based ferroelectric crystals. Nature Communications, 2022, 13, 2444.	12.8	46
14	Antiferroelectric Phase Diagram Enhancing Energy-Storage Performance by Phase-Field Simulations. ACS Applied Materials & Interfaces, 2022, 14, 25770-25780.	8.0	7
15	Electric-Field-Insensitive Temperature Stability of Strain in KNN Multilayer Composite Ceramics. ACS Applied Materials & Interfaces, 2022, 14, 26949-26957.	8.0	8
16	Response to Comment on $\hat{a} \in \infty$ Improper molecular ferroelectrics with simultaneous ultrahigh pyroelectricity and figures of merit $\hat{a} \in \mathbf{s}$ Science Advances, 2022, 8, .	10.3	0
17	Strain manipulation of ferroelectric skyrmion bubbles in a freestanding <mml:math xmlns:mml="http://www.w3.org/1998/Math/MathML"> <mml:msub> <mml:mi>PbTiO </mml:mi> <mml:mn>3 film: A phase field simulation. Physical Review B, 2022, 105, .</mml:mn></mml:msub></mml:math 	ml:m2> <td>nmlømsub> <</td>	nmlømsub> <
18	Phase-Field Model of Hydride Blister Growth Kinetics on Zirconium Surface. Frontiers in Materials, 2022, 9, .	2.4	3

2

#	Article	IF	CITATIONS
19	High-entropy enhanced capacitive energy storage. Nature Materials, 2022, 21, 1074-1080.	27.5	161
20	Enhancing the Elastocaloric Strength by Combining Positive and Negative Elastocaloric Effects. Physica Status Solidi - Rapid Research Letters, 2022, 16, .	2.4	1
21	Ferroelectric domain-wall logic units. Nature Communications, 2022, 13, .	12.8	37
22	Designing Ultrafast Cooling Rate for Room Temperature Electrocaloric Effects by Phaseâ€Field Simulations. Advanced Theory and Simulations, 2022, 5, .	2.8	4
23	Quantitative investigation of polar nanoregion size effects in relaxor ferroelectrics. Acta Materialia, 2022, 237, 118147.	7.9	5
24	Explicit Dynamics of Diffuse Interface in Phaseâ€Field Model. Advanced Theory and Simulations, 2021, 4, .	2.8	4
25	Multi-phase-field simulation of austenite peritectic solidification based on a ferrite grain*. Chinese Physics B, 2021, 30, 018201.	1.4	2
26	Core–Shell Magnetic Micropillars for Reprogrammable Actuation. ACS Nano, 2021, 15, 4747-4758.	14.6	30
27	Visualization of large-scale charged domain Walls in hexagonal manganites. Applied Physics Letters, 2021, 118, .	3.3	4
28	Toroidal polar topology in strained ferroelectric polymer. Science, 2021, 371, 1050-1056.	12.6	74
29	Large Room Temperature Negative Electrocaloric Effect in Novel Antiferroelectric PbHfO ₃ Films. ACS Applied Materials & Interfaces, 2021, 13, 21331-21337.	8.0	21
30	Designed Giant Roomâ€Temperature Electrocaloric Effects in Metalâ€Free Organic Perovskite [MDABCO](NH ₄)I ₃ by Phase–Field Simulations. Advanced Functional Materials, 2021, 31, 2104393.	14.9	27
31	Phase-field simulations of surface charge-induced ferroelectric vortex. Journal Physics D: Applied Physics, 2021, 54, 405302.	2.8	9
32	Defectâ€Engineered Dzyaloshinskii–Moriya Interaction and Electricâ€Fieldâ€Switchable Topological Spin Texture in SrRuO ₃ . Advanced Materials, 2021, 33, e2102525.	21.0	34
33	Defectâ€Engineered Dzyaloshinskii–Moriya Interaction and Electricâ€Fieldâ€&witchable Topological Spin Texture in SrRuO ₃ (Adv. Mater. 33/2021). Advanced Materials, 2021, 33, 2170255.	21.0	1
34	Hydride corrosion kinetics on metallic surface: a multiphase-field modeling. Materials Research Express, 2021, 8, 106518.	1.6	3
35	A parabolic approximation scheme for multi-phase-filed simulation of non-isothermal solidification. Materials Today Communications, 2021, 28, 102712.	1.9	0
36	Ultrahigh energy storage in superparaelectric relaxor ferroelectrics. Science, 2021, 374, 100-104.	12.6	276

#	Article	IF	CITATIONS
37	Polarization-switching pathway determined electrical transport behaviors in rhombohedral BiFeO ₃ thin films. Nanoscale, 2021, 13, 17746-17753.	5.6	7
38	Improper molecular ferroelectrics with simultaneous ultrahigh pyroelectricity and figures of merit. Science Advances, 2021, 7, .	10.3	32
39	How Far Can We Push the Rigid Oligomers/Polymers toward Ferroelectric Nematic Liquid Crystals?. Journal of the American Chemical Society, 2021, 143, 17857-17861.	13.7	36
40	High-entropy polymer produces a giant electrocaloric effect at low fields. Nature, 2021, 600, 664-669.	27.8	121
41	Phase-field simulation of multi-phase interactions in Fe-C peritectic solidification. Computational Materials Science, 2020, 171, 109220.	3.0	15
42	Multiphase-field approach with parabolic approximation scheme. Computational Materials Science, 2020, 172, 109322.	3.0	8
43	Influences of grain/particle interfacial energies on second-phase particle pinning grain coarsening of polycrystalline. Journal of Alloys and Compounds, 2020, 818, 152848.	5.5	19
44	Influences of particle fractions on second-phase particles pinning grain coarsening processes. Journal of Materials Science, 2020, 55, 3434-3449.	3.7	5
45	Determining dendrite arm spacing in directional solidification using a fast Fourier transform method. Computational Materials Science, 2020, 173, 109463.	3.0	6
46	Phase-field simulation of two-dimensional topological charges in nematic liquid crystals. Journal of Applied Physics, 2020, 128, 124701.	2.5	2
47	The strong electrocaloric effect in molecular ferroelectric ImClO ₄ with ultrahigh electrocaloric strength. Journal of Materials Chemistry A, 2020, 8, 16189-16194.	10.3	23
48	Theoretically optimized hybrid magnetic nanoparticle concentrations for functional gradient nanocomposites. AIP Advances, 2020, 10, 105209.	1.3	1
49	Phase-field model of topological charge interaction force in nematic liquid crystals. Soft Materials, 2020, , 1-6.	1.7	0
50	Domain wall tuned superconductivity in superconductor–ferromagnet bilayers. Journal Physics D: Applied Physics, 2020, 53, 375001.	2.8	2
51	Hybrid Magnetic Micropillar Arrays for Programmable Actuation. Advanced Materials, 2020, 32, e2001879.	21.0	58
52	Ferroelasticâ€Domainâ€Assisted Mechanical Switching of Ferroelectric Domains in Pb(Zr,Ti)O ₃ Thin Films. Advanced Electronic Materials, 2020, 6, 2000300.	5.1	12
53	Fe-C peritectic solidification of polycrystalline ferrite by phase-field method. Computational Materials Science, 2020, 178, 109626.	3.0	8
54	Domain evolution in bended freestanding BaTiO3 ultrathin films: A phase-field simulation. Applied Physics Letters, 2020, 116, .	3.3	15

#	Article	IF	CITATIONS
55	Investigation into electrocaloric effect of different types of ferroelectric materials by Landau-Devonshire theory. Wuli Xuebao/Acta Physica Sinica, 2020, 69, 217801.	0.5	8
56	Phase field simulation of misfit strain manipulating domain structure and ferroelectric properties in PbZr _(1–<i>x</i>) Ti <i>_x</i> O ₃ thin films. Wuli Xuebao/Acta Physica Sinica, 2020, 69, 127801.	0.5	4
57	Tunable temperature dependence of electric-field-control multicaloric effects. Journal of Alloys and Compounds, 2019, 806, 1491-1496.	5.5	4
58	Super-elastic ferroelectric single-crystal membrane with continuous electric dipole rotation. Science, 2019, 366, 475-479.	12.6	272
59	Size-Dependent Phase Transition in Perovskite Nanocrystals. Journal of Physical Chemistry Letters, 2019, 10, 5451-5457.	4.6	48
60	Phase-field model of graphene aerogel formation by ice template method. Applied Physics Letters, 2019, 115, 111901.	3.3	11
61	Current assisted memory effect in superconductor–ferromagnet bilayers: a potential candidate for memristors. Superconductor Science and Technology, 2019, 32, 095002.	3.5	5
62	Wide Electrocaloric Temperature Range Induced by Ferroelectric to Antiferroelectric Phase Transition. Applied Sciences (Switzerland), 2019, 9, 1672.	2.5	10
63	Phase-field simulations of surface charge-induced polarization switching. Applied Physics Letters, 2019, 114, .	3.3	15
64	Grain boundary curvature based 2D cellular automata simulation of grain coarsening. Journal of Alloys and Compounds, 2019, 791, 411-422.	5.5	18
65	Strain-induced broadening temperature range of electrocaloric effects in ferroelectric superlattices. Journal of Alloys and Compounds, 2019, 777, 821-827.	5.5	12
66	Boundary Pinning Effects on the Frequency Spectra of Point-Contact Spin-Torque Oscillators. IEEE Magnetics Letters, 2018, 9, 1-4.	1.1	1
67	Role of Reversible Phase Transformation for Strong Piezoelectric Performance at the Morphotropic Phase Boundary. Physical Review Letters, 2018, 120, 055501.	7.8	84
68	Numerical Simulation of Phase Transitions in Type-II Annular Superconductor Using Time-dependent Ginzburg-Landau Equations. Journal of Superconductivity and Novel Magnetism, 2018, 31, 3445-3451.	1.8	7
69	Size effects of electrocaloric cooling in ferroelectric nanowires. Journal of the American Ceramic Society, 2018, 101, 1566-1575.	3.8	38
70	Effect of Background Magnetic Field on Type-II Superconductor under Oscillating Magnetic Field Simulated Using Ginzburg-Landau Model. Advances in Condensed Matter Physics, 2018, 2018, 1-7.	1.1	0
71	Understanding and predicting geometrical constraint ferroelectric charged domain walls in a BiFeO3 island via phase-field simulations. Applied Physics Letters, 2018, 113, .	3.3	17
72	Switching the chirality of a magnetic vortex deterministically with an electric field. Materials Research Letters, 2018, 6, 669-675.	8.7	13

#	Article	IF	CITATIONS
73	Water printing of ferroelectric polarization. Nature Communications, 2018, 9, 3809.	12.8	75
74	Bioinspired Wearâ€Resistant and Ultradurable Functional Gradient Coatings. Small, 2018, 14, e1802717.	10.0	14
75	High electrocaloric effect in hotâ€pressed Pb _{0.85} La _{0.1} (Zr _{0.65} Ti _{0.35})O ₃ ceramics with a wide operating temperature range. Journal of the American Ceramic Society, 2017, 100, 4581-4589.	3.8	30
76	Magnetically actuated functional gradient nanocomposites for strong and ultra-durable biomimetic interfaces/surfaces. Materials Horizons, 2017, 4, 869-877.	12.2	28
77	Simulation of stress-modulated magnetization precession frequency in Heusler-based spin torque oscillator. Journal of Magnetism and Magnetic Materials, 2017, 426, 415-420.	2.3	3
78	Micromagnetic simulation of electric field-modulation on precession dynamics of spin torque nano-oscillator. Applied Physics Letters, 2017, 111, .	3.3	4
79	Numerical simulation of vortex dynamics in type-II superconductors in oscillating magnetic field using time-dependent Ginzburg–Landau equations. Journal of Physics Condensed Matter, 2017, 29, 505701.	1.8	8
80	Nanoscale Bandgap Tuning across an Inhomogeneous Ferroelectric Interface. ACS Applied Materials & Interfaces, 2017, 9, 24704-24710.	8.0	14
81	Thickness Dependence of Switching Behavior in Ferroelectric BiFeO3 Thin Films: A Phase-Field Simulation. Applied Sciences (Switzerland), 2017, 7, 1162.	2.5	10
82	Simulation of Magnetically-Actuated Functional Gradient Nanocomposites. Applied Sciences (Switzerland), 2017, 7, 1171.	2.5	2
83	Micromagnetic Simulation of Strain-Assisted Current-Induced Magnetization Switching. Advances in Condensed Matter Physics, 2016, 2016, 1-6.	1.1	2
84	Multi-scale simulations of metamagnetic martensite transition in NiCoMnIn. Journal of Alloys and Compounds, 2016, 689, 507-511.	5.5	5
85	Toward Wearable Cooling Devices: Highly Flexible Electrocaloric Ba _{0.67} Sr _{0.33} TiO ₃ Nanowire Arrays. Advanced Materials, 2016, 28, 4811-4816.	21.0	101
86	Analysis of multi-domain ferroelectric switching in BiFeO3 thin film using phase-field method. Computational Materials Science, 2016, 115, 208-213.	3.0	18
87	Magnetization switching modes in nanopillar spin valve under the external field. Science China: Physics, Mechanics and Astronomy, 2011, 54, 1227-1234.	5.1	8